GIS-MODELED MORPHOMETRY OF DARK-HALO CRATERS IN ALPHONSUS CRATER. M. A. Hunter, L. R. Gaddis, L. P. Keszthelyi, and L. Glaspie, USGS Astrogeology Science Center, Flagstaff, AZ 86004 (mahunter@usgs.gov, lgaddis@usgs.gov, laz@usgs.gov, lglaspie@usgs.gov).

Introduction: Alphonsus crater is well known for the dark-halo craters originating from vents in its floor. These localized, low albedo deposits are volcanic in origin and have been studied in the past to constrain the timing, duration and modes of lunar pyroclastic emplacement events. Wilson and Head's 1979 volumetric study [1] was performed on 1:50,000-scale topographic maps from Apollo 16 panoramic camera images. The availability of higher resolution base maps, digital elevation models (DEM) and spectral data make it possible to perform the similar analyses with improved precision in a geographic information system (GIS) [2].

This geospatial analysis underpins our group's ongoing research into lunar pyroclastic deposits. Alphonsus contains 11 dark-halo craters sourced from rilles in varying topographic settings on the crater floor [3]. This study has refined measurements made initially by Wilson and Head [1], and was expanded to capture metrics needed for modeling emplacement of these pyroclastic eruptions [4]. A subset of the original sites was used in this study, including dark-halo craters Alphonsus R, Ravi and Soraya (***Figure 1***).

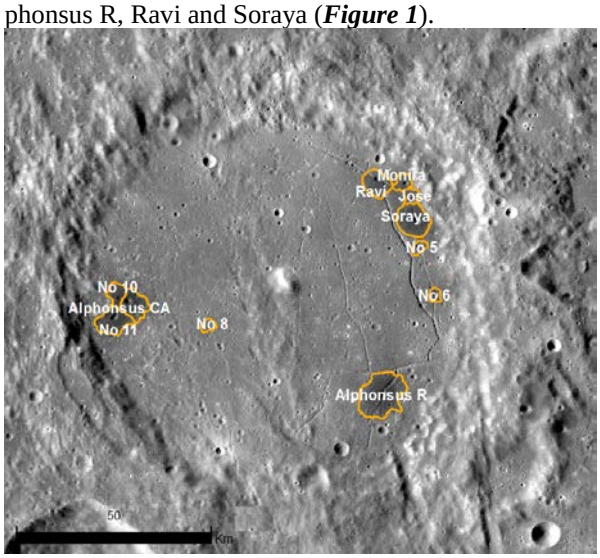

Figure 1. Alphonsus crater, with digitized dark-halo crater boundaries on the LRO WAC 100 mpp mosaic.

Methodology: Datasets used include the merged Lunar Orbiter Laser Altimeter (LOLA) / SELenological and Engineering Explorer (SELENE) "Kaguya" Terrain Camera (TC) DEM (60 mpp; known as "SLDEM2015") [5], Lunar Reconnaissance Orbiter (LRO) Wide Angle Camera (WAC) mosaic (100 mpp), Kaguya Multi-Band Imager 750 nm Reflectance map (237 mpp), and Clementine UVVIS Color Ratio map (200 mpp). Crater halos were digitized based on albedo, topography, and color data, while crater rims and centers were digitized based on a DEM-derived "flow direction" map (part of the hydrology toolset, the *Flow Direction* tool integrates slope and aspect data into one map). Rilles were digitized with five lines at their edges, walls and center from topographic data, except for smaller branch rilles which used three lines. These methods are similar to those used previously [6], but refined to use higher resolution data and calculate more robust statistics.

Reconstruction of Pre-Eruptive Surface. The clipped DEM was converted to points, with post spacing equal to the raster resolution, and all points inside the halo were deleted. The rilles were converted to points with 60 m spacing, and merged into the DEM-derived point feature class. Rille points were then attributed with elevations sampled from the exposed rille floor outside of the crater halo. This was converted to a triangulated irregular network (TIN), using Delaunay conforming triangulation to interpolate the gaps between elevation between halo and rille edges. The TIN was then converted to a raster at the same resolution as SLDEM2015, and snapped to the original cell alignment (***Figure 2***).

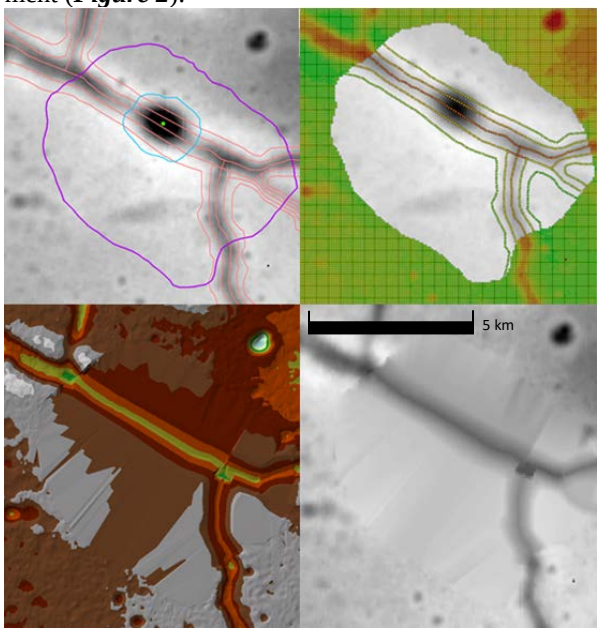

Figure 2. Views of Ravi (read top-left to bottom-right). Digitized crater halo, rim, center and rilles; ele-

vation points; TIN derived from points; pre-eruptive surface DEM.

Crater Volumetrics and Statistics. With both DEMs clipped to the shape of the crater halo the *Cut/Fill* tool was used to calculate the amount of material excavated from the vent and deposited. These measures were used to calculate the amount of juvenile material added to the observed deposit volume and to estimate deposit thicknesses [3].

Crater statistics were then calculated to leverage the full resolution of the data, using a variety of ArcMap geoprocessing routines. For example, by converting the crater halo to points with 60 m spacing the *Distance to Points* tool provided the minimum, maximum and mean of the halo radius sampled at DEM resolution. A difference map was also created from the two DEMs, using *Raster Calculator*, which provided pre- and post-eruption measures at the rilles, crater floor, center and rim.

Profile Data for Ballistic Model. The final step of the analysis was to created multi-directional profiles of the craters (***Figure 3***), and extract underlying layer data for use in a tabular model. This entailed the digitization of four profile lines crossing through the crater center and extending beyond the halo edge. New fields were then added to the profile lines, including "Directionality" (i.e., "NW-SE"), "In_Out" (status inside or outside of halo), "Elevation", "Reflectance", "X" and "Y". Then the lines were converted to points with 60 m spacing. The *Extract Multiple Values to Points* tool was used to extract values from the DEM and Kaguya Reflectance map, and the coordinate fields were populated with the *Calculate Geometry* attribute field option. Exported as a *.csv file, the resulting tables were sorted by directionality, longitude and latitude for use with other key metrics in Keszthelyi's lunar ballistic model [4].

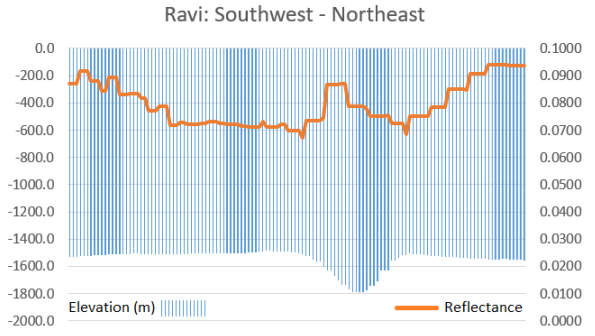

Figure 3. Example plot of the southwest – northeast profile of Ravi; note the difference in resolution between elevation (60 mpp) and reflectance (237 mpp).

Results: Of the three sites studied here, Alphonsus R was not part of Wilson and Head's initial work, and was measured to have the lowest percentage of juvenile material at 28%. The others, Ravi and Soraya, resulted in overall percentages of juvenile material closer to earlier values. Ravi, originally measured as 58% juvenile material, was refined to 75%, and Soraya saw a shift from 90% to 80%. Preliminary review of results suggests that degradation of vents over time and local topography significantly influence volume measurements. These site were selected because they were less affected by adjacent vents and the local topography, but many other sites are located in more complex terrain.

Future Work: The goal of this work is to improve our characterization of the likely energetics, volatile content, eruptive styles, durations, and compositional phases of the Alphonsus deposits. This methodology will be applied to other sites, and may be revisited as higher resolution data of the region becomes available. For example, Gaddis et al. [3] have identified additional, previously unrecognized dark-halo crater candidates for study within Alphonsus.

Future work will include exploration of methods for more accurately reconstructing the pre-eruptive surface (such as 3-D visualization of halo edges for more precise digitization), and testing of interpolation methods. The relatively thin mantling and diffuse boundaries of dark-halo craters are difficult to discern from topography alone, so multi-variate raster classification methods may be of great benefit as well. We also intend to implement a version of our simple crater eruption model [4] that allows us to integrate compositional and topographic data in a 3D rendering and to more readily interpret relationships between observed distribution of minerals around the Alphonsus vents [7].

The ability to harness the full resolution of new products makes GIS an ideal environment for testing new analysis methods, and development of tools for modeling interactions between ejecta and topography. Such tools may become invaluable for supporting larger-scale investigations of volcanic eruptions on the Moon and other Solar System bodies.

References: [1] Head J. W. and Wilson L. (1979) *Proc. LPS Conf. 10th*, 2861-2897. [2] Gaddis L. R. et al. (2011) LPS XLII, Abstract #1608. [3] Gaddis L. R. et al. (2018) LPS XLIX, this meeting. [4] Keszthelyi L. P. et al. (2018) LPS XLIX, this meeting. [5] Barker M. K. et al. (2016) *Icarus*, *273*, 346-355. [6] Skinner Jr, J. A. et al. (2005) LPS XXXVI, Abstract #2344. [7] Glaspie L. et al. (2018)LPS XLIX, this meeting.